Desalination and Water Treatment
www.deswater.com

41 (2012) 53–61
March

doi: 10.1080/19443994.2012.664678

Taylor & Francis
Taylor & Francis Group

Synthesis of new modified MCM-41/PSF nanocomposite membrane for improvement of water permeation flux

Abolfazl Jomekian[a,*], Alireza Shafiee[b], Amin Moradian[b]

[a]*Department of Chemical Engineering, Faculty of Engineering, Ferdowsi University of Mashhad,*
P.O. Box 91775-1111, Mashhad, Iran
Fax: +98 511 6220302; email: abolfazl.jomekian@gmail.com
[b]*Department of Chemical Engineering, Sharif University of Technology, Tehran, Iran*

Received 9 December 2010; Accepted 10 January 2012

ABSTRACT

The preparation of MCM-41 nanoparticles was made using tetraethylorthosilicate as silica source and cetyltrimethylammonium bromide as surfactant. The X-ray diffraction, transmission electron microscopy, laser particle size analysis and N_2 adsorption techniques were used for characterization of nanoparticles. The dimethyldichlorosilan (DMDCS) was applied to improve the dispersion of MCM-41 nanoparticles into the polysulfone (PSF) matrix. The investigation on the thermal stability with thermogravimetric analysis showed the enhanced stability of membranes possessing higher loading of MCM-41 nanaoparticles. The scanning electron microscopy was used to evaluate the quality of particles dispersion and the result showed that the modification of MCM-41 particles by DMDCS caused good quality dispersion of particles in to the polymer matrix. In order to enhance the hydrophilicity of MCM-41 nanoparticles, modification by ethylene diamine was performed. Permeation performance of the prepared membranes was evaluated in terms of water content (WC) and pure water flux (PWF) and NaCl salt rejection. The WC of modified membranes increased compared to unmodified and neat polymeric membranes. The membranes, PWF permeation test showed that addition of modified MCM-41 nanoparticles led to increase in water permeation. The adequate NaCl, Na_2SO_4, and $CaCl_2$ salt rejection indicated that the nanofilteration process incorporating MCM-41 particles into the matrix of PSF is a promising candidate for desalination applications. The rejection results indicate that the charge (Donnan) exclusion mechanism is the dominant effect resulting in high salt rejection.

Keywords: Modified MCM-41; Polysulfone; DMDCS; Ethylene diamine; Water content; Pure water flux

1. Introduction

The demands for water and protection of the entire ecosystems are an important issue credited to the entire world's population. On one side, the development of new materials with advanced properties such as high pore volume, specific surface area, open pore systems, thermal and hydrothermal stability, given monomodal particles is an ongoing task for many environmentally friendly chemical processes [1–5].

Water sorption behavior in nanoporous materials plays an important role in manufacturing and designing of advanced materials and devices thereafter. The

---

*Corresponding author.

most studied adsorbents for water are microporous materials (zeolites), activated carbon, and silica gels [6,7]. Despite the fact that they are efficient in many cases, they do not have the specific surface area and pore volume as much as mesoporous materials.

Mesoporous compounds are another group of materials with potential applications as water sorbents synthesized by using long-chain surfactant molecules as templates [5,8,9]. The common MCM-41, MCM-48, MCM-50, FSM-16, KIT-1, SBA-2, and SBA-15 materials have different pore sizes (2–10 nm), large surface areas (>500 m^2/g), and variable dimensions and shapes. The mesoporous semi-crystalline compounds are expected to exhibit adsorption characteristics different from ordinary silica gels. The mesoporous materials, regardless of the structure, type, and composition have abundant number of silanol groups because of the amorphous surface structure. Therefore, a large amount of water can be sorbed on them followed by capillary condensation [10–15].

The MCM-41 is one of the most useful materials due to the structural simplicity (uniform cylindrical/hexagonal pore channels with very narrow pore size distribution), and easy pathway of preparation with negligible pore-blocking effects [16–18]. Apart from that, the high thermal, hydrothermal, chemical, and mechanical stability are highly conducive for a number of important applications such as adsorption and separation.

To synthesize a composite organic/inorganic membrane, the polysulfone with characteristics such as good toughness, high biocompatibility, good desalting, high potential flux, and relatively low cost has been chosen as a polymeric matrix [19–21].

Clearly the success of the polymer nanocomposite membranes depends largely on the quality of the interface between the nanofiller and the polymer [22]. Inagaki et al., Long et al., and Zhao et al. believe that the siliceous mesoporous materials are classified as hydrophobic materials since they sorb more organics than water but they also believe that with some modification by a hydrophilicity increaser agent this problem could be solved satisfactory [23–26]. Kim et al. [27,28] enhanced the permeability of PSF by incorporating mesoporous MCM-48.

Nanoscale molecular sieves are more suitable for commercialization of nanocomposite membranes whereas they have very thin selective layers than micron-sized zeolites or molecular sieves. Recently, the additional functionalization of nanofiller surface in order to enhance sorption effects of these particles and provide proper adherence between inorganic and organic phases has been considered by researchers [29,30].

In this study, as a new work, the functionalization of particles was performed by dimethyldichlorosilane (DMDCS) as a new modification agent to make the particles to disperse widely into the matrix of polymer and the hydrophilicity of MCM-41 particles was enhanced by engulfing them in the ethylene diamine. The main purpose of this study is the fabrication and characterization of a new modified MCM-41/PSF nanocomposite membrane in order to gain the superior capacity for water sorption. In the first step, MCM-41 nanoparticles were produced and then their structures were investigated with several adequate characterization methods containing particle size analysis, X-ray diffraction (XRD) analysis, pore size analysis, and transmission electron microscopy (TEM). The effect of inorganic nanofiller on thermal stability nanocomposite membranes was studied by thermogravimetric analysis (TGA). The scanning electron microscopy (SEM) was used to investigate the quality of modified obtained nanocomposite membranes. Finally, the sorption and permeation performance of prepared nanocomposite membranes was evaluated by water content (WC) and pure water flux (PWF), and salt rejection measurement tests.

2. Experimental

2.1. Synthesis and functionalization of MCM-41 nanoparticles

The nanoparticles of MCM-41 were synthesized through the self-assembly of inorganic silica precursor and organic template. The source of silicon was tetraethylorthosilicate (TEOS, Merck). The structure-directing agent was cetyltrimethylammonium bromide (CTAB, Merck). A typical synthesis gel was prepared by adding 5.78 g of TEOS to an aqueous solution containing 1.01 g of CTAB, 0.34 g of NaOH, and 30 ml of deionized water. After stirring for about 2 h at room temperature, the resulting homogeneous mixture was crystallized under static hydrothermal conditions at 373 K in a homemade Teflon-lined autoclave for 72 h. The molar composition of the initial gel mixture was 1.0:0.10:0.30:60 TEOS/CTAB/NaOH/H_2O. The solid product was obtained by filtration, washed with deionized water, dried in vacuum oven at 353 K, and calcined in air at 833 K for 10 h with 1°C/min of heating rate to remove the CTAB. This method results in the unmodified version of MCM-41 nanoparticles [27]. As shown in Fig. 1, surface modification of MCM-41 particles was performed this way: before removing CTAB, silylation of MCM-41 with dimethylsilane was achived by the immersion of MCM-41 nanoparticles

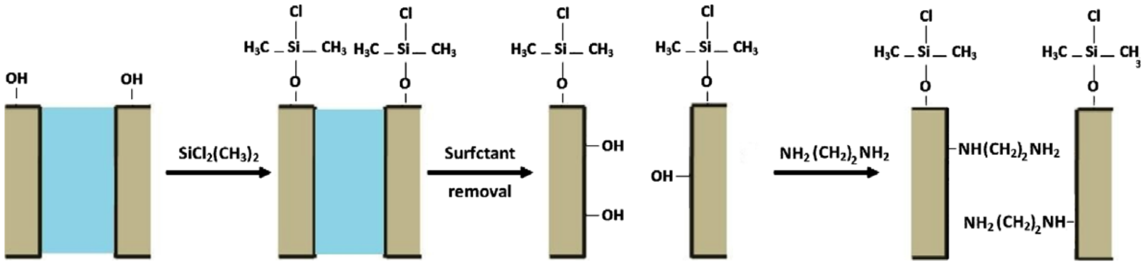

Fig. 1. Silylation and amine treatment of MCM-41 nanoparticles.

into liquid DMDCS (Merck) for 72 h and then for about 24 h in the ethylene diamine. Afterwards CTAB was removed by means of soxhlet extraction apparatus using 300 ml of methanol and 30 ml of aqueous HCl (10% vol). The extraction process was continued for about 24 h then the mixture was filtered and washed with 200 ml of ethanol and in the end the modified mesoporous MCM-41 samples were filtered and washed in soxhlet apparatus with n-hexane, and then dried at 333 K in oven [28].

2.2. Synthesis of membranes

Before using PSF (Ultrason 6010, Merck) powder in synthesis process, it must be degassed at 423 K for 2 h under vacuum to remove all of its WC. To prepare a sample of MCM-41/PSF nanocomposite membrane, 1.2 g of the pure PSF was dissolved in 6 ml of N,N-dimethylacetamide (DMAc, Merck) and mixed for 12 h then for making 10 wt.% of MCM-41 in the PSF solution, 0.1 g of MCM-41 powder was dissolved in N,N-dimethylacetamide with a few drops of PSF solution and sonicated in ultrasonic bath for about 20 min. After that, this MCM-41 solution was added to the polymer solution and the mixture was allowed to mix for 4 h at room temperature then the mixture was sonicated for 10 min, after which it was allowed to mix for 10 min and this procedure repeated several times to ensure perfect dispersion. The prepared casting solution was cast on a glass substrate using casting blade. The glass substrate was covered with a glass cover to slow down the evaporation rate of the solvent, allowing for the formation of a film with a uniform thickness without curling. After about 1 min, the glass substrate was placed into a coagulation bath of deionized water. Coagulation of film immediately occurred and the membrane formed and separated from glass substrate. The membrane remained in deionized water bath for about 24 h to complete the phase separation process then dried in air at 323 K.

2.3. Characterization

Powder XRD data were recorded using a Philips Analytical X-pert diffractometer with Cu Ka radiation ($\lambda = 1.54056$ Å) with a step size of 0.02 °/s. N_2 adsorption isotherms were measured at 77 K on a Micromeritics ASAP 2010 analyzer using standard continuous procedures. Samples were first degassed at 573 K for 5 h. Surface areas and pore size distribution were determined by BET and BJH methods, respectively [31,32]. The particle size analysis for MCM-41 particles was performed by means of Shimadzu sald-2101. SEM (LEO 1450VP) was used to study the morphology of the membranes. The transmission electron micrographs (TEM) were obtained on a Zei (LEO912AB) transmission electron microscope device. Thermal stability of membrane was investigated by TGA in Shimadzu (TGA-50/50h) by heating at a rate of 3°C /min up to 600°C. WC of the membranes was obtained after soaking membranes in water for 24 h and the membranes were weighed followed by mopping them with blotting paper. The wet membranes were placed in vacuum drier at 75°C for 48 h and the dry weights of the membranes were determined [33]. The percent of WC was calculated using the equation:

$$WC\% = \frac{(W_{wet} - W_{dry})}{W_{wet}} \times 100 \qquad (1)$$

where W_{wet} and W_{dry} are the wet and dry weights of the membranes, respectively.

A membrane pilot containing a disk membrane module made from stainless steel was used in the experiments. The effective membrane area in the module is 35 cm^2. The schematic representation of membrane pilot is shown in Fig. 2. The PWF measurement was carried out in a batch mode and transmembrane pressure of 1 bar. PWF is calculated using the following equation:

$$PWF = \frac{Q}{A} \qquad (2)$$

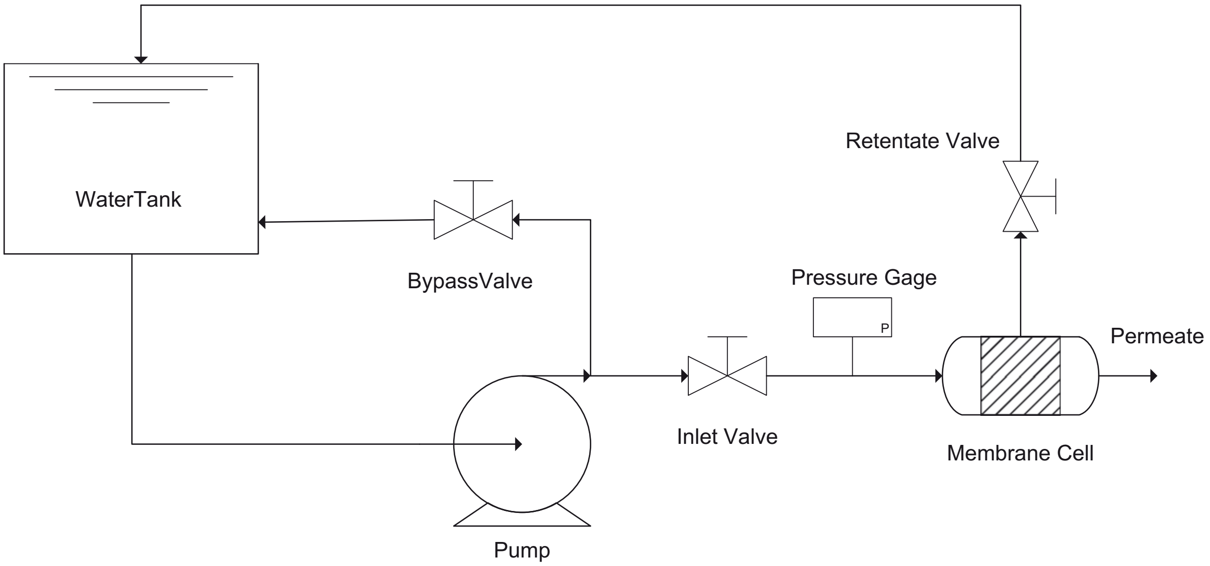

Fig. 2. Schematic diagram of membrane pilot.

where Q is the permeate volumetric flow rate and A is the effective membrane area.

At each time interval, the feed and permeate were sampled, and the selectivity was determined by measuring the ion rejection (R_i), that is, the ratio of the ion concentration in the permeate to that in the feed:

$$R_i(\%) = \frac{C_{i,F} - C_{i,P}}{C_{i,F}} \times 100 \tag{3}$$

where $C_{i,F}$ and $C_{i,P}$ are the concentrations of solute i in the feed and permeate, respectively.

The salt concentrations were evaluated by ion chromatography (IC; ICS-1500, Dionex, USA) and inductively coupled plasma spectrometry (ICP; Optima 5300DV ICP-OES, Perkin Elmer, USA).

3. Results and discussion

3.1. Characterization results of MCM-41 nanoparticles

The XRD pattern of the mesoporous material is shown in Fig. 3. The observation of several Bragg peaks at low reflection angles ($2\theta = 2.5$–7.0), which are relevant to (1 0 0), (1 1 0), (2 0 0), and (2 1 0) and can be indexed in a hexagonal lattice and correspond well to the hexagonally arranged pore structure of MCM-41, is the proof of a long-range order and consequently of the good quality of the sample. As the material is not crystalline at the atomic level, no reflections at higher angles are observed.

The particle size analysis result of modified MCM-41 in Fig. 4 shows that the congeries of particles' sizes is mostly between 40 and 90 nm and this proves the nanoscale structure of produced MCM-41 particles.

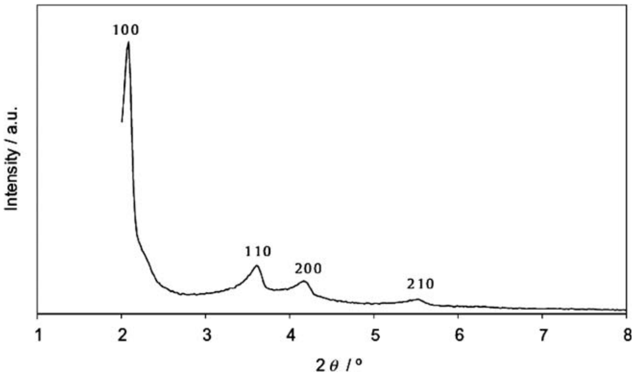

Fig. 3. XRD pattern of MCM-41 particles.

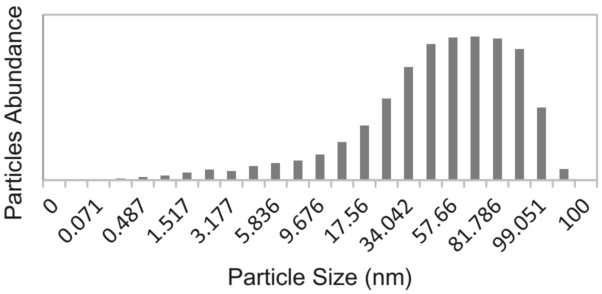

Fig. 4. The particle size distribution of MCM-41 nanoparticles.

The nitrogen adsorption–desorption isotherm of extracted MCM-41 at 77 K exhibits both a reversible type IV isotherm and a sharp pore filling step at p/p_0 0.2–0.3 which are characteristic of uniform pores (Fig. 5). The sample shows high specific surface area, approximately 930 m^2/g, and a narrow distribution of pore diameters centered at 2.2 nm (Fig. 6) which confirms results of the XRD analysis.

The TEM images of the modified MCM-41 particles in Fig. 7 show the existence of ordered hexagonal structures with pore sizes of about 2–2.5 nm. These XRD patterns, pore size analysis, and TEM results are in agreement with previously published results on nano-sized mesoporous silica materials [34,35].

3.2. Characterization results of MCM-41/PSF nanocomposite membranes

3.2.1. Scanning electron microscopy

The formation of undesirable gaps or aggregation of inorganic particles in the polymer may happen because of incompatibility between the polymer and the inorganic material, deducing the sorption capability and mechanical properties of the membrane.

In order to investigate the quality of dispersion of MCM-41 nanoparticles into the polymer matrix, we utilized SEM images of surface of two kinds of nanocomposite membranes, filled with unmodified MCM-41 and contained silylated MCM-41. SEM surface images of 20 wt.% unmodified and DMDCS-modified MCM-41/PSF nanocomposite membranes are shown in Fig. 8. Fig. 8(a) shows that in the unmodified MCM-41 case in which the unfavorable voids between polymer matrix and inorganic particles present, one can see the agglomeration of particles. However, as can be seen in Fig. 8(b), the DMDCS-modified MCM-41 nanoparticles are well dispersed in the PSF matrix and the distinct voids between two phases cannot be distinguished. The reason for these two different kinds of behaviors is due to silanol groups' function. Since they have hydrophobic property and the surface of unmodified MCM-41 nanocomposite membrane is covered by them, the MCM-41 particles easily adhere to each other via hydrogen bonding and form irregular agglomeration in the polymer matrix. However, in the modified version, the surface of membrane is silylated with dimethylsilyl and ethylene diamine groups hence the hydrophobic surface of membrane turns to hydrophilic surface. This treatment prevents the particles from being agglomerated and enhances the interaction between particles and polymer producing a composite with well-dispersed mesoporous particles in the polymer matrix. This trend also can be seen in Fig. 9, in this figure the porous structure of membrane is clearly shown.

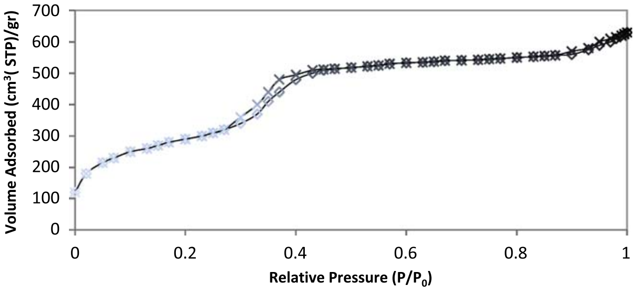

Fig. 5. The N_2 adsorption–desorption isotherms of MCM-41 particles at 77 K.

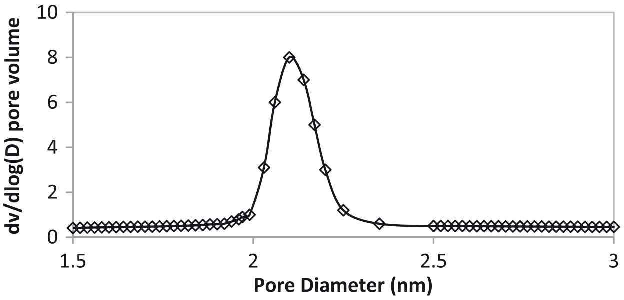

Fig. 6. The pore size distribution of MCM-41 particles.

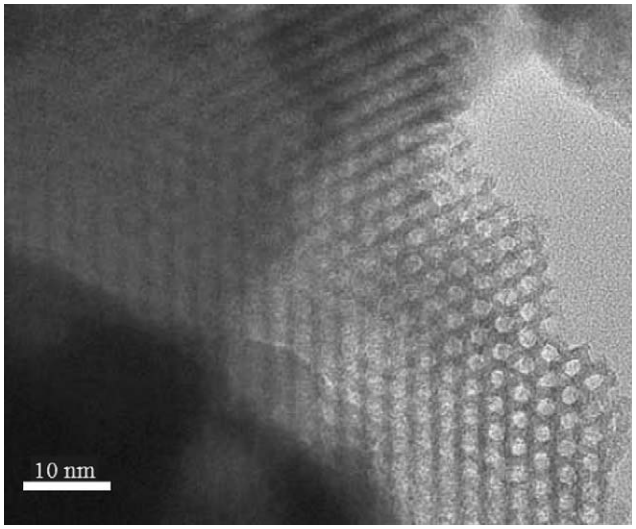

Fig. 7. The TEM image of MCM-41 pores.

The pores of membrane are about 3–5 μm and the uniformity of the pore sizes shows that the coagulation bath of deionized water successfully created these pores. The other concept that can be inferred from this cross-sectional SEM image is that the thickness of the membrane is about 40–50 μm which demonstrates that the membrane is thin enough that it can enhance the water permeation flux and the resistance preventing the water from passing the membrane is low.

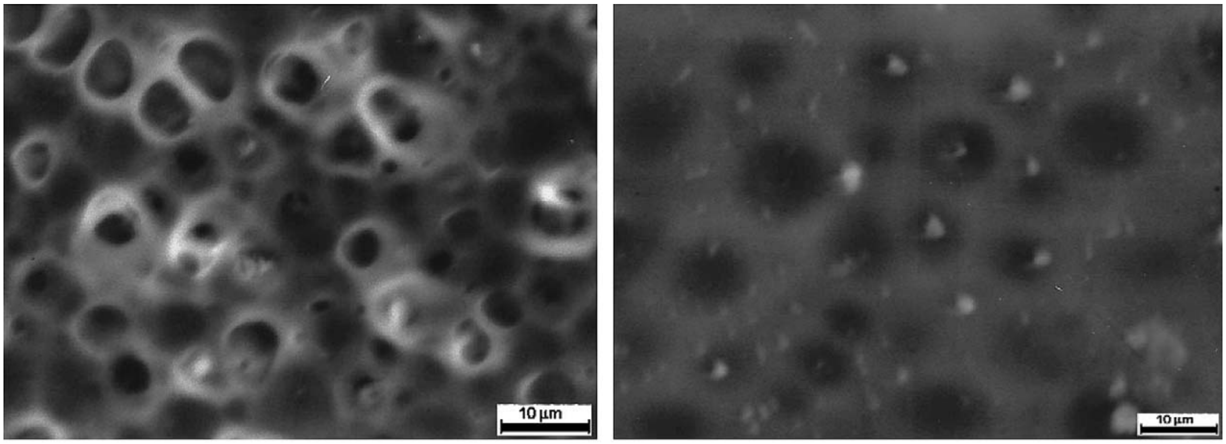

(a) (b)

Fig. 8. SEM images of (a) unmodified and (b) DMDCS-modified MCM-41/PSF composite membrane.

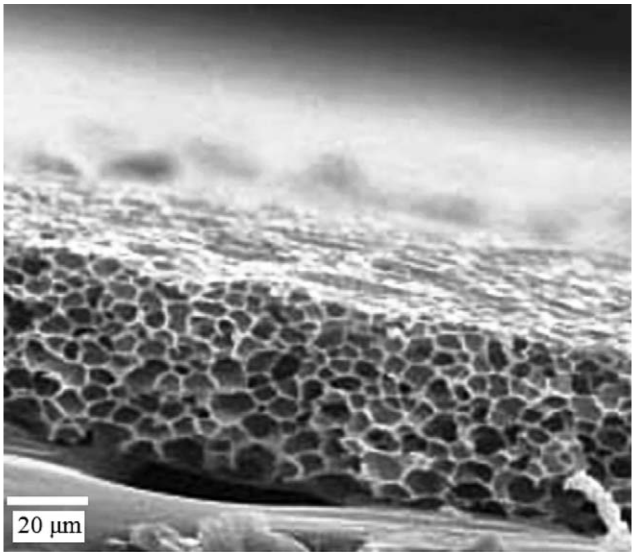

Fig. 9. Cross-sectional SEM image of DMDCS modified MCM-41/PSF nanocomposite membranes.

3.2.2. Thermogravimetric analysis

As can be seen in Fig. 10, TGA results obtained from three samples with 10 wt.%, 20 wt.%, and 40 wt.% MCM-41 loading show that the thermal stability of membrane remarkably enhances with increasing the MCM-41 loading in the polymer matrix. The 10 wt.% membrane has a good thermal stability till 445°C then loses weight. However, the 20 wt.% and 40 wt.% MCM-41 loaded membranes have thermal stability till 500°C and 560°C respectively. These results demonstrate that by increasing the loading of thermally stable inorganic MCM-41 into the polymer matrix, the degradation temperature of membrane rises and the thermal stability of membrane significantly improves.

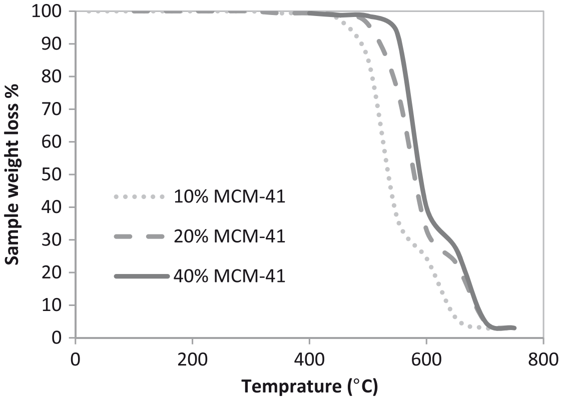

Fig. 10. TGA thermodiagrams of MCM-41/PSF composite membranes with different MCM-41 loading.

3.2.3. Water content

WC is related to the membrane hydrophilic property [36]. WC of each membrane is calculated using Eq. (1). As Table 1 shows, WC for pure PSF is equal to 63.75, whereas for the PSF nanocomposite membrane with 40 wt.% of unmodified MCM-41 and DMDCS modified nanoparticles it is equal to 79.47 and 84.51, respectively.

It is obvious that WC is increased by increasing the weight percent of MCM-41 nanoparticles. Severance of polymer chains due to the presence of MCM-41 nanoparticles creates the spaces in the polymer matrix which leads to increasing the WC. The well-dispersed nanoparticles of the modified version of MCM-41 make its WC increase more than that of unmodified version. The good dispersion of particles in the polymer matrix enhances the specific surface area and pore volume of particles and so increases the

Table 1
Effect of MCM-41 nanoparticles on WC of each membrane

Membrane	MCM-41 (wt.%)	WC (%)
PSF	0	63.75
U^{a} MCM41/PSF	10	65.99
DM^{b} MCM41/PSF	10	68.12
U MCM-41/PSF	20	72.58
DM MCM41/PSF	20	77.32
U MCM41/PSF	40	79.47
DM MCM41/PSF	40	84.51

[a] U = unmodified.
[b] DM = DMDCS modified.

water sorption capacity of modified sample compared to unmodified sample.

3.2.4. Pure water flux

The addition of modified MCM-41 nanoparticles can influence the PWF at least in two features. At first it causes that the membrane becomes more hydrophilic. The contact angle measurement proves this claim properly (Fig. 11). As can be seen, the contact angle of pure PSF membrane (membrane with no MCM-41 loading) is about 74°. By increasing the MCM-41 loading, the contact angle data of unmodified membranes increased; meaning the hydrophobicity of the membranes was enhanced with the addition of MCM-41 nanoparticles. This could be associated with the hydrophobicity of MCM-41 particles.

Compared with unmodified versions of membranes and pure PSF membrane, amin modified membranes have lower contact angle, meaning the hydrophilicity of the membranes was improved with modification by ethylene diamine. Secondly its effect on the membrane morphology affects its permeation properties. The relationship of PWF of the membranes against MCM-41 nanoparticles amount is presented in Fig. 12. In general, the PWF is increased by increasing the MCM-41 amount in the casting solution and reached a maximum value of 62.36 L/m^2 h when the MCM-41 amount is 20 wt.%. At 10 wt.% and 20 wt.% of MCM-41 nanoparticles, the MCM-41 nanoparticles quite dispersed into the matrix of polymer and water is allowed to pass through MCM-41 channels easily and so, it increases the flux. At 40 wt.% of MCM-41 nanoparticles, the relative agglomeration of nanoparticles on the membrane matrix leads to the little decrease of PWF.

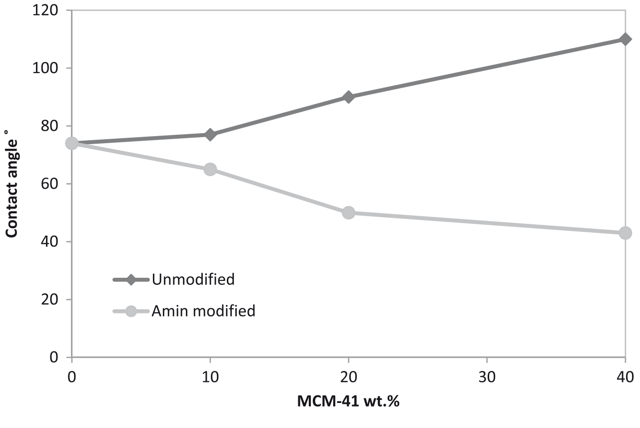

Fig. 11. Contact angle of PSF membranes synthesized with different loading of unmodified and modified MCM-41.

3.2.5. Salt rejection measurement

The ion concentrations on the feed and permeate sides along with the ion rejections in the water desalination tests are listed in Tables 2 and 3. As can be seen in Tables 2 and 3, with enhancement in MCM-41 loading in the polymer matrix the ion rejection percent increases. The other fact that can be seen in the tables is that the ion rejection by the unmodified nanocomposite membranes is obviously lower than those by modified membranes. This might be due to the agglomeration of number of unmodified MCM-41 particles in the matrix of PSF that create the unfavorable shortcut for passing the ions.

Salt rejection through nanoporous nanocomposite membranes can be attributed to size exclusion or charge exclusion or surface evaporation. In the size exclusion mechanism, the hydrated radius and hydration shells are important. Ions are hydrated in water, so their hydrated radii are much larger than the radii of bare ions. The dependency of the anion rejections on the hydrated diameter and the rapid rejection reversals assisted in the size exclusion mechanism as well. Therefore, it could be concluded that the size

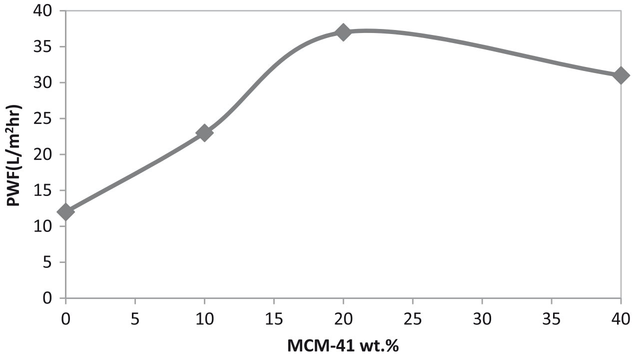

Fig. 12. Effect of MCM-41 amount on membranes PWF.

Table 2
Na^+ concentration on feed and permeate sides during NF

Membrane	MCM-41 (wt.%)	Conc. feed (ppm Na^+)	Conc. permeate (ppm Na^+)	Rejection (%)
PSF	0	6,410	495.7	92.3
U[a] MCM41/PSF	10	6,503	866.96	86.6
DM[b] MCM41/PSF	10	6,503	278.3	95.7
U MCM-41/PSF	20	6,570	794.41	87.9
DM MCM41/PSF	20	6,570	207.6	96.8
U MCM41/PSF	40	6,692	949.80	85.8
DM MCM41/PSF	40	6,692	203.2	96.9

[a] U = unmodified.
[b] DM = DMDCS modified.

Table 3
Cl^- concentration on feed and permeate sides during NF

Membrane	MCM-41 (wt.%)	Conc. feed (ppm Cl^-)	Conc. permeate (ppm Cl^-)	Rejection (%)
PSF	0	7,894	447.1	94.3
U MCM41/PSF	10	7,789	1,536.5	80.3
DM MCM41/PSF	10	7,789	318.1	95.9
U MCM-41/PSF	20	7,771	1,264.93	83.7
DM MCM41/PSF	20	7,771	232.8	97.0
U MCM41/PSF	40	7,836	1,330.16	83.0
DM MCM41/PSF	40	7,836	219.7	97.2

exclusion mechanism was also operative in the present system.

The rejection (%) comparison of Na_2SO_4, NaCl, and $CaCl_2$ solutions vs. water permeate flux indicated in Fig. 13 shows that the more negative charge of ions leads to higher rejection (%) and also the more positive charge results in lower rejection (%). According to these observations it can be concluded that the Donnan (charge) exclusion is also a serious effect in high rejection outcome. The enhancement of rejection (%) with increase in water permeation flux is probably due to the "dilution effect" that makes the concentration of ions to decrease [37].

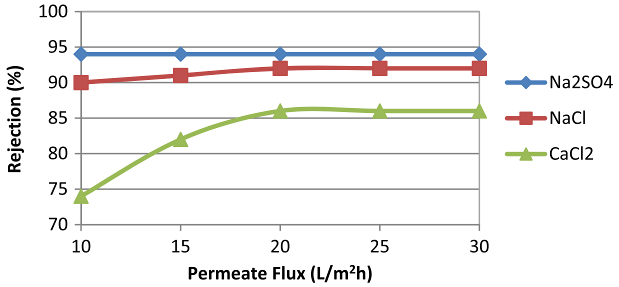

Fig. 13. Rejection of salt solution vs. water permeate flux.

4. Conclusion

Mesoporous MCM-41 was synthesized and modified by DMDCS to incorporate into the matrix of PSF in order to enhance the WC and PWF of nanocomposite membrane. The TGA results show improvement of thermal stability of PSF by introducing MCM-41 nanoparticles into it. The SEM results show the better dispersion of modified MCM-41 nanoparticles in the matrix of polymer compared to the unmodified one. Results from WC test show that by increasing the concentration of MCM-41 nanoparticles in the casting solution, the water sorption capacity of membrane increases and the sorption capacity of modified version of membranes is higher than unmodified versions. Permeation performance of the modified nanocomposite membranes was also greatly improved because of the addition of MCM-41 nanoparticles. The membrane with maximum flux was obtained when the MCM-41 amount was 20 wt.%. The ion rejection tests showed that the enhancement in MCM-41 loading in the matrix of PSF increased the rejection (%) and showed that the modification of MCM-41 nanoparticles effectively enhanced the rejection (%) of the ions tested.

References

[1] R.W. Baker, Membrane Technology and Application, John Wiley & Sons Ltd., Chichester, 2004.

[2] R.D. Noble and S.A. Stern, Membrane Separation Technology, Principles and Applications, Elsevier, Amsterdam, 1995.

[3] R. Singh, Hybrid Membrane Systems for Water Purification, Elsevier, Oxford, 2006.

[4] T.C. Merkel, B.D. Freeman, R.J. Spontak, Z. He, I. Pinnau, P. Meakin, A.J. Hill, Ultrapermeable, reverse-selective nanocomposite membranes, Science 296 (2002) 519–522.

[5] C.T. Kresge, M.E. Leonowics, W.J. Roth, J.C. Vartulli, J.S. Beck, Ordered mesoporous molecular sieves synthesized by a liquid-crystal template mechanism, Nature 359 (1992) 710–712.

[6] J.P. Boom, I.G.M. Punt, H. Zwijnenberg, R. de Boer, D. Bargeman, C.A. Smolders, H. Strathmann, Transport through zeolite filled polymeric membranes, J. Membrane Sci. 138 (1998) 237–258.

[7] B. Moermans, W.D. Beuckelaer, I.F.J. Vankelecomm, R. Ravishankar, J.A. Martens, P.A. Jacobs, Incorporation of nano-sized zeolites in membranes, Chem. Commun. (2000) 2467–2468.

[8] J.S. Beck, J.C. Vartuli, W.J. Roth, M.E. Leonowics, C.T. Kresge, K.D. Schmitt, C.T.W. Chu, D.H. Olson, E.W. Sheppard, S.B. McCullen, J.B. Higgings, J.L. Schlenker, A new family of mesoporous molecular sieves prepared with liquid crystal templates, J. Am. Chem. Soc. 114 (1992) 10834–10843.

[9] K. Moller, T. Bein, Inclusion chemistry in periodic mesoporous hosts, Chem. Mater. 10 (1998) 2950–2963.

[10] J.F. Diaz, K.J. Balkus, Enzyme immobilization in MCM-41 molecular sieve, J. Mol. Catal. B Enzym. 2 (1996) 115–126.

[11] W. Xu, Q. Luo, H. Wang, L.C. Francesconi, R.E. Stark, D.L. Akins, Polyoxoanion occluded within modified MCM-41: Spectroscopy and structure, J. Phys. Chem. B 107 (2003) 497–501.

[12] P.L. Llewellyn, U. Ciesla, H. Decher, R. Stadler, F. Schueth, K.K. Unger, MCM-41 and related materials as media for controlled polymerization processes, Stud. Surf. Sci.Catal. 84 (1994) 2013–2020.

[13] A. Corma, V. Forne´ s, M.T. Navarro, J. Pe´ rez-Patiente,, J. Pe´ rez-Patiente, Acidity and stability of MCM- 41 crystalline aluminosilicates, J. Catal. 148 (1994) 569–574.

[14] M. Raimondo, G. Perez, M. Sinibaldi, A. De Stefanis, A.A.G. Tomlinson, Mesoporous M41S materials in capillary gas chromatography, Chem. Commun. 15 (1997) 1343–1344.

[15] L. Sierra, B. Lopez, J.L. Guth, Preparation of mesoporous silica particles with controlled morphology from sodium silicate solutions and a non-ionic surfactant at pH values between 2 and 6, Micropor. Mesopor. Mater. 39 (2000) 519–527.

[16] J. Mapkar, G. Iyer, M. Coleman, Functionalization of carbon nanofibers with elastomeric block copolymer using carbodiimide chemistry, Appl. Surf. Sci. 255 (2009) 4806–4813.

[17] J. Xu, W. Chu, S. Luo, Synthesis and characterization of mesoporous V-MCM-41 molecular sieves with good hydrothermal and thermal stability, J. Mol. Catal. A: Chem. 256 (2006) 48–56.

[18] H.K. Shon, S. Puntsho, K. Chon, R. Aryal, S. Vigneswaran, S. Kim, J. Cho, A study on the influence of ionic strength on the elution behaviour of membrane organic foulant using advanced separation tools, J. Deswater 11 (2009) 38–45.

[19] S.C. Pesek, W.J. Koros, Aqueous quenched asymmetric polysulfone membranes prepared by dry/wet phase separation, J. Membr. Sci. 81 (1993) 71–88.

[20] R.L. McGinnis, M. Elimelech, Energy requirements of ammonia–carbon dioxide forward osmosis desalination, Desalination 207 (2007) 370–382.

[21] G.C. Kapantaidakis, S.P. Kaldis, X.S. Dabou, G.P. Sakellaropoulos, Gas permeation through PSF-PImiscible blend membranes, J. Membr. Sci. 110 (1996) 239–252.

[22] V.Y. Gusev, X. Feng, Z. Bu, G.L. Haller, J.A. O'Brien, Mechanical stability of pure silica mesoporous MCM-41 by nitrogen adsorption and small-angle X-ray diffraction measurements, J. Phys. Chem. 100 (1996) 1985–1988.

[23] S. Inagaki, Y. Fukushima, Adsorption of water vapor and hydrophobicity of ordered mesoporous silica, FSM-16, Micropor. Mesopor. Mater. 21 (1998) 667–672.

[24] Y. Long, T. Xu, Y. Sun, W. Dong, Adsorption behavior on defect structure on mesoporous molecular sieve MCM-41, Langmuir 14 (1998) 6173–6178.

[25] X.S. Zhao, G.Q. Lu, Modification of MCM-41 by surface sylylation with trimethylchlorosilane and adsorption study, J. Phys. Chem. B 102 (1998) 1556–1561.

[26] H. Sijbesma, K. Nymeijer, R. vanMarwij, R. Heijboer, J. Potreck, M. Wessling,, Flue gas dehydration using polymer membranes, J. Membr. Sci. 313 (2008) 263–276.

[27] S. Kim, E. Marand, J. Ida, V.V. Guliants, Polysulfone and mesoporous molecular sieve MCM-48 mixed matrix membranes for gas separation, Chem. Mater. 18 (2006) 1149–1155.

[28] S. Kim, E. Marand, High permeability nano-composite membranes based on mesoporous MCM-41 nanoparticles in a polysulfone matrix, Micro. Meso. Mater. 114 (2008) 129–136.

[29] A. Tuel, S. Gontier, Synthesis and characterization of trivalent metal containing mesoporous silicas obtained by a neutral templating route, Chem. Mater. 8 (1996) 114–122.

[30] M. Jaroniec, M. Kruk, H.J. Shin, R. Ryoo, Y. Sakamoto, O. Terasaki, Comprehensive characterization of highly ordered MCM-41 silicas using nitrogen adsorption, thermogravimetry, X-ray diffraction and transmission electron microscopy, Micropor. Mesopor. Mater. 48 (2001) 127–134.

[31] S. Kim, J. Ida, V.V. Guliants, Y.S. Lin, Tailoring surface properties of MCM-48 silica by bonding 3-aminopropyltriethoxysilane for selective adsorption of carbon dioxide, J. Phys. Chem. B 109 (2005) 6287–6293.

[32] S. Brunauer, P.H. Emmett, E. Teller, Adsorption of gases in multimolecular layers, J. Am. Chem. Soc. 60 (1938) 309–319.

[33] M. Sivakumar, A.K. Mohansundaram, D. Mohan, K. Balu, R. Rangarajan, Modificationof CA: Its characterization and application as an UF membranes, J. Appl. Polym. Sci. 67 (1998) 1939–1946.

[34] Floreta Constantinescu., Jana Blum, Adsorption characterisation of the dealumination effect on H-mordenites, J. Porous Mater. 2 (1995) 35–41.

[35] Q. Cai, Z.S. Luo, W.Q. Pang, Y.W. Fan, X.H. Chen, F.Z. Cui, A simple route for preparing radiolarian-like mesoporous silica from water–diethyl ether binary solvent system, Chem. Mater. 13 (2001) 258–263.

[36] M. Sivakumar, D. Mohan, R. Rangarajan, Studies on cellulose acetate/polysulfone ultrafiltration membranes II: Effect of additive concentration, J. Membr. Sci. 268 (2006) 208–219.

[37] A. Seidel, J.J. Waypa, M. Elimelech, Role of charge (Donnan) exclusion in removal of arsenic from water by a negatively charged porous nanofiltration membrane, Environ. Eng. Sci. 18 (2001) 105–113.